Ab-Initio X-Ray Powder Structure Analysis of Two Polymorphs of Dihydroxysilicon Phthalocyanine

Yuko Kojima,* Yasuko T. Osano, and Toyoshi Ohashi

Yokohama Research Center, Mitsubishi Chemical Corporation, 1000, Kamoshida-cho, Aoba-ku, Yokohama 227-8502

(Received May 6, 1999)

This paper reports on the synthesis and ab-initio X-ray powder structure determination of two polymorphs of [Si-(OH)$_2$Pc], where Pc = phtalocyaninato. We found that one of the polymorphs (Phase II) shows high sensitivity for an electrophotographic photoreceptor, but that the other (Phase I) doesn't have photosensitivity. The difference in the sensitivity depends on only the crystal structures. This material has not been able to be grown to a single crystal with sufficient size for single crystal X-ray analysis, but it is very important to determine the crystal structures of the two polymorphs for understanding the mechanism of the performance of the electrophotographic photoreceptor. In this work we carried out ab-initio X-ray powder structure analysis. The compound crystallizes in space group $P\bar{1}$ (Phase I), $Z = 1$ with unit-cell parameters of $a = 12.992(1)$, $b = 7.2830(8)$, $c = 6.861(1)$ Å, $\alpha = 104.413(7)°$, $\beta = 101.757(8)°$, $\gamma = 96.973(6)°$ and in space group $P2_1/n$ (Phase II), $Z = 2$ with unit-cell parameters of $a = 12.7494(5)$, $b = 14.5778(6)$, $c = 6.7727(3)$ Å, $\beta = 94.353(2)°$. Both phases have symmetry center in the molecules (on Si atom) and intermolecular hydrogen bonds (O–H···N). These hydrogen bond modes of Phase I and Phase II are the same. The main difference in packings was revealed between the crystals: Phase II crystal has the herringbone structure, while in Phase I all molecules form the parallel stack columns.

Phthalocyanines have been studied for electrophotographic photoreceptors of long wavelength sensitivity. They are extremely stable pigments and exhibit many photochemical properties. In addition to a wide variety of central metals, there are also many polymorphs. It is known that some of the polymorphs of titanyloxyphthalocyanine in particular have high sensitivity in the near-infrared region.[1] Titanylphthalocyanine [TiOPc], which is a rigid molecule, has been found to have four polymorphs (Phases A, B, C, D); the photochemical activities depend on only the crystal structures (sensitivity: Phase D > Phase A ≫ Phase B ≫ Phase C).[2] We believe that the molecular packing or stacking determines the photochemical properties. It is expected that there are more active and stable crystalline materials in many phthalocyanines with various metals.

We recently, found that dihydroxysilicon phthalocyanine [Si(OH)$_2$Pc][3] has two polymorphs, and that one of them (Phase II) is an efficient photocarrier generating pigment, while the other (Phase I) is not. Phase I is more stable than Phase II in the solid state, Phase II transforms to Phase I by mechanochemical process. This phenomenon suggests that the molecular packings of the two polymorphs have some common featuer. It would be interesting to clarify the relationship between the crystal structures and the photochemical sensitivity.

Unfortunately, the two polymorphs of Si(OH)$_2$Pc have never been grown in sufficiently large crystals for the single crystal analysis, just like many other phthalocyanines polymorphs. However, in order to clarify the photochemical properties of the phthalocyanines it is very important to obtain the crystal structures. We have thus tried the crystal structure analysis from powder X-ray diffraction data. It is known that the organic crystal structure determination from powder diffraction data is very difficult due to low symmetry and large cell constants compared with the one of inorganic compounds. There are some cases in which information concerning a known single crystal structure of another polymorph is used to solve the crystal structure from powder X-ray diffraction data.[4] In this work we report on complete ab-initio X-ray powder structure analysis of two phases of Si(OH)$_2$Pc based on synchrotron X-ray powder diffraction measurement. The results of this analysis show the key information of how to rationalize the charge carrier generation and crystal stability.

Experimental

Synthesis. The samples (Phase I & Phase II) of Si(OH)$_2$Pc were prepared from SiCl$_2$Pc via different routes. Phase I was synthesized from SiCl$_2$Pc directly and Phase II was prepared via Si(OMe)$_2$Pc. The reactions leading to the two polymorphs of [Si(OH)$_2$Pc] are given in Scheme 1.

SiCl$_2$Pc. 43.5 g of 1,3-diiminoisoindoline and 73.5 g of silicon tetrachloride were added to 500 ml of quinoline and reacted at 210 to 220 °C for 1 h under a nitrogen atmosphere. The reaction product

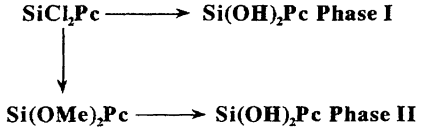

Scheme 1.

was thermally filtrated at 180 °C and washed with quinoline and acetone in the order named. After the product was heated under reflux in 300 ml of acetone, the crystalline powder was separated by filtration and dried to obtain 38.7 g of dichlorosilicon phthalocyanine. In IR spectrum, absorption characteristic to dichlorosilicon phthalocyanine was observed at 1533, 1079, and 1060 cm^{-1}.[5]

Si(OH)$_2$Pc Phase I. 20 g of dichlorosilicon phthalocyanine was added to a mixture solution of 5 g of NaOH, 250 ml of water and 50 ml of pyridine and reacted under reflux for 2 h. The reaction product was then thermally filtrated and washed with water, and methanol in the order named. The crystalline powder was separated by filtration and dried to obtain 18.2 g of dihydroxysilicon phthalocyanine (Phase I).

Si(OMe)$_2$Pc. 10 g of dichlorosilicon phthalocyanine was added to a mixture solution of 1.86 g of sodium methoxide, 100 ml of methanol and 100 ml of pyridine and reacted under reflux for 3 h. The reaction product was thermally filtrated and washed with methanol, water, and acetone in the mentioned order. Thereafter, it was washed in 100 ml of water several times, its neutralization was confirmed, and the crystalline powder was separated by filtration and dried to obtain 9.7 g of dimethoxysilicon phthalocyanine.

Si(OH)$_2$Pc Phase II. 10 g of dimethoxysilicon phthalocyanine was added to 5 g of water and 95 g of *N*-methyl-2-pyrrolidone (95% NMP aqueous solution) and reacted at 120 °C for 3 h. The reaction product was thermally filtrated and washed with NMP, and acetone in the mentioned order. After the product was stirred in 100 ml of acetone at room temperature, the crystalline powder was separated by filtration and dried to obtain 8.0 g of dihydroxysilicon phthalocyanine (Phase II).

Analytical. Figure 1 shows the mass spectrum and the IR spectrum of Si(OH)$_2$Pc (Phase II). In the mass spectrum, which was measured with a JEOL JMS-700 mass spectrometer using the desorption chemical ionization method, a main peak of Si(OH)$_2$Pc

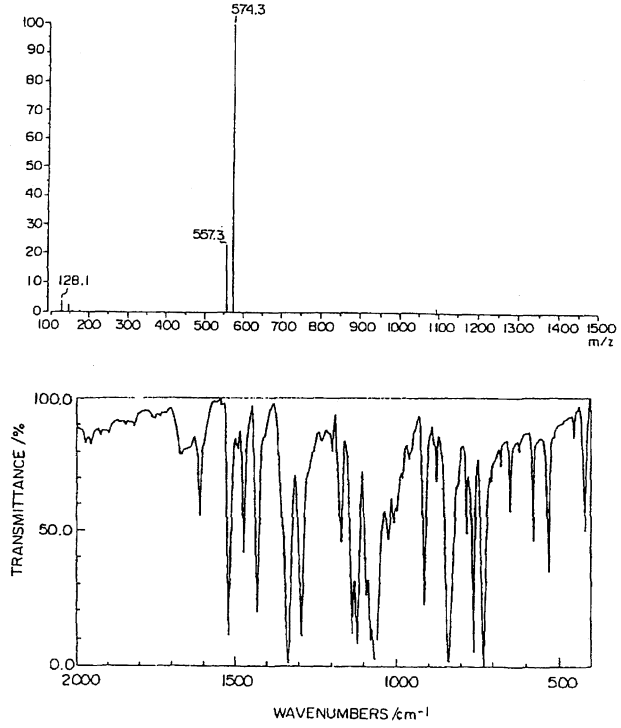

Fig. 1. The mass spectrum (upper) and the IR spectrum (lower) of Si(OH)$_2$Pc (Phase II).

cation was observed at an *m/z* of 574. A sub-peak at an *m/z* of 557 is a fragment peak of the compound from which one hydroxy group is removed. In the IR spectrum that was recorded with a Horiba FT-210 infrared spectrophotometer, the absorption characteristic to Si(OH)$_2$Pc was observed at 1519, 1066, and 839 cm^{-1}.[5] The results of the elemental analysis of Phase II are Found: C, 65.70; H, 3.10; N, 19.10; Si, 4.94%. Calcd for $C_{32}H_{18}N_8O_2Si$: C, 66.89; H, 3.16; N, 19.50; Si, 4.89%. The spectrum and the elemental analysis of Phase I were very similar to those of Phase II. It was thereby confirmed that the synthesized products were Si(OH)$_2$Pc.

The dark blue powder were gently ground in an agate mortar, then cautiously deposited in a flat aluminium sample holder and mounted on an X-ray diffractometer (Rigaku-MDS). The samples were rotated at 60 rpm about the scattering vector, in order to minimize the preferred orientation effects. The powder X-ray diffraction data were collected at room temperature at the 4Ab beam line of Synchrotron Light Source, KEK. X-rays of wavelength 1.5406 Å were selected by Si(111) monochromator and confirmed using the reference peaks of Si powder (NBS640b). Data were taken for 2.5 s at each 2θ in steps of 0.005° (from 5° to 75° 2θ). Figure 2 shows the raw XRPD data for the two phases.

Indexing the reflections was tried using ITO,[6] DICVOL,[7] TREOR,[8] and an original program. These attempts with low-angle 20 peaks suggested a triclinic cell having approximate dimensions of a = 13.03, b = 7.30, c = 6.88 Å, α = 104.3°, β = 101.7°, γ = 97.0° for Phase I and a monoclinic cell having approximate dimensions of a = 12.75, b = 14.61, c = 6.79 Å, β = 94.4° for Phase II. The density values (1.56 g cm^{-3}, Z = 1 for Phase I and 1.51 g cm^{-3}, Z = 2 for Phase II) calculated from these cell constants are quite consistent with those (1.57 g cm^{-3} for Phase I and 1.52 g cm^{-3} for Phase II) obtained by measurement with the Helium substitution method. In the case of Phase II, it is so very difficult to obtain the cell constant from only the powder peaks that we ascertained the solution from the Synchrotron X-ray Polaroid spots of a micro-single crystal (a few micron) that was a grain of the powder. This picture (Fig. 3) shows the a^*b^* plane of the reciprocal lattice.

The space group of Phase I is $P1$ or $P\bar{1}$. It was determined from the crystal system and unit-cell volume. Systematic absences for Phase II, which were obtained from electron diffraction patterns (Fig. 4), indicated existence of two-fold screw axis ($0k0$ $k = 2n+1$). Also, it was expected that the space group of Phase II is $P2_1$ or $P2_1/n$. In both Phases if the crystals have symmetry center, the molecules have symmetry center themselves, because of the results concerning the crystal density.

We used the molecular model to solve the crystal structures, which was made from the results of single crystal analysis of the similar phthalocyanine.[9] Figure 5 shows the molecular model in this analysis, which has symmetry center on Si atom and H atoms are omitted. Si atom is at the center of the phthalocyanine plane and two hydroxy fragments are bonded to the Si atom upper and lower side of the plane (∠O–Si–O 180°. The space groups were finally determined to be $P\bar{1}$ for Phase I and $P2_1/n$ for Phase II based on molecular symmetry. We carried out Rietveld analysis[10] while assuming that the shape of the molecule is rigid.

In order to obtain the initial crystal structures of Rietveld refinement we tried two different methods. First, we put the molecule in the unit cells and calculated the X-ray pattern. The coordinate of the Si atom was fixed at the origin of the unit cell by crystal and molecular symmetry restraint. We then rotated the molecules in the unit cells and selected the initial structures having the most similar X-ray pattern with the observation. Second, we carried out molecular mechanics calculation with PCK91.[11,12] In both Phases most stable

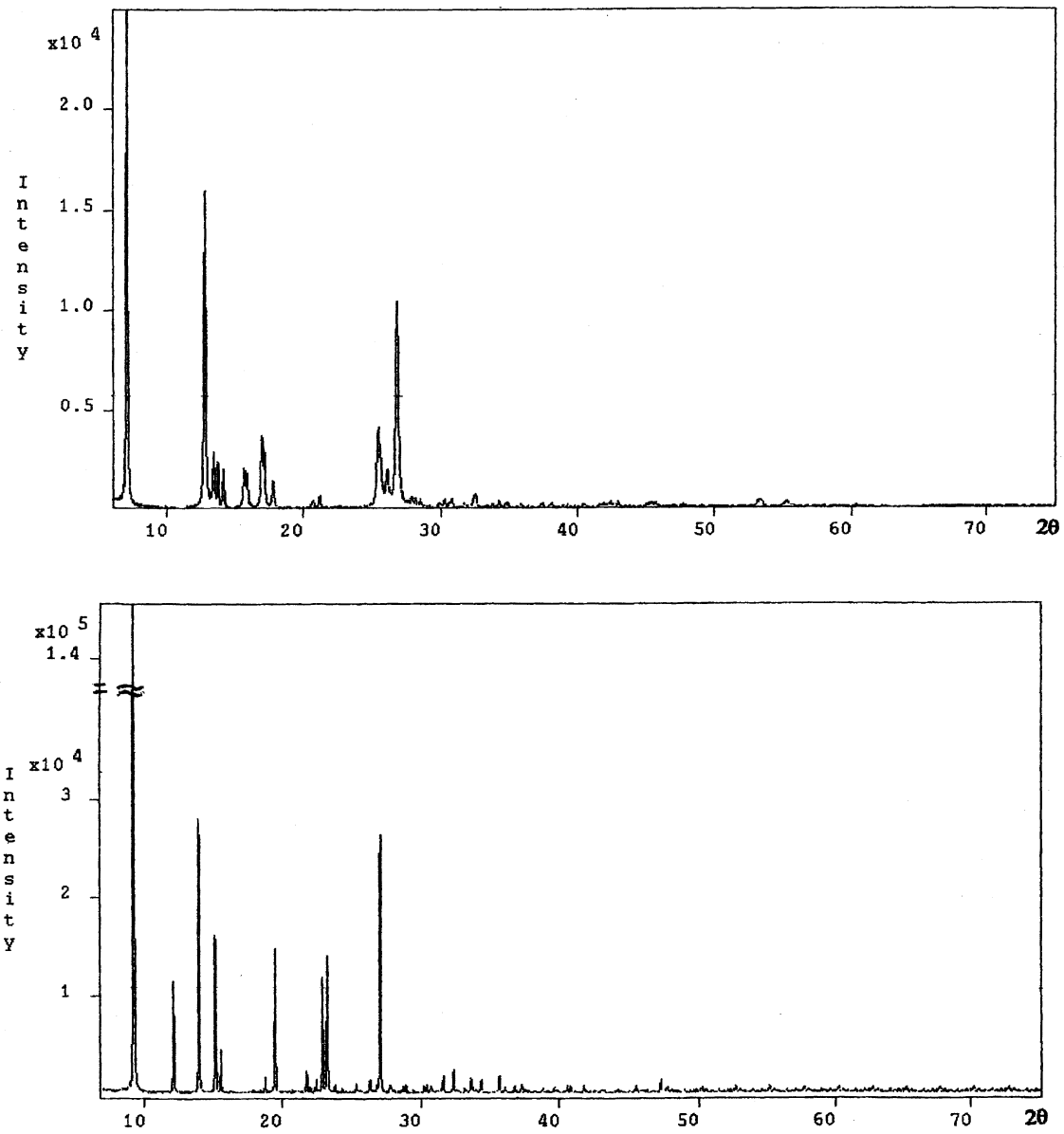

Fig. 2. Raw XRPD data for $Si(OH)_2Pc$: Phase I (upper) and Phase II (lower).

structures are considered to be the initial structures. Fortunately, the results from the two methods were almost the same.

Final Rietveld refinements were performed with the program RIETAN,[13,14] and the results are shown in Fig. 6. Scale factor, unit-cell parameters, zero-shift error, background parameters, peak profile parameters, and preferred orientation parameters were refined. The Si atom that was fixed at the origin of the unit cell and the coordinates of the other non-H atoms were also refined as rigid bodies. The isotropic temperature factors of all non-H atoms were not refined. H atoms were not included in the calculations. The peak profile function was modeled using a multiterm Simpson's rule integration of the pseudo-Voigt function.[15] The Modified Marquadt method was used for the least-squares calculations. The final R values and the crystal data are listed in Table 1. The fractional coordinates using rigid bodies are given in Table 2. A selection of the intermolecular distances and angles including hydrogen bonds is given in Table 3.

Measurement of the Electric Properties. The initial electric properties (charge potential, dark decay, half-decay exposure sensitivity, residual potential) of the obtained photoreceptor (Phase I & Phase II) were evaluated using an electrostatic copy paper testing machine (Model EPA-8100 of Kawaguchi Denki Seisakusho Co.). The photoreceptor was negatively charged by corona discharge for 2.4 s at an application voltage which was set to ensure that the corona current should be 22 μA in the dark (the surface potential at this point was taken as the charge potential). Then, the negatively charged photoreceptor was continuously exposed to 1.0 $\mu W\,cm^{-2}$ monochromatic light having a wavelength of 780 nm for 10 s to measure the attenuation of the surface potential (the surface potential after 10 s of exposure was taken as residual potential). The reducing potential one second after charging was taken as the dark decay; the amount of exposure ($E_{1/2}$) required to reduce surface potential from −450 to −225 V was taken as the half-decay exposure sensitivity (= sensitivity). The results are given in Table 4.

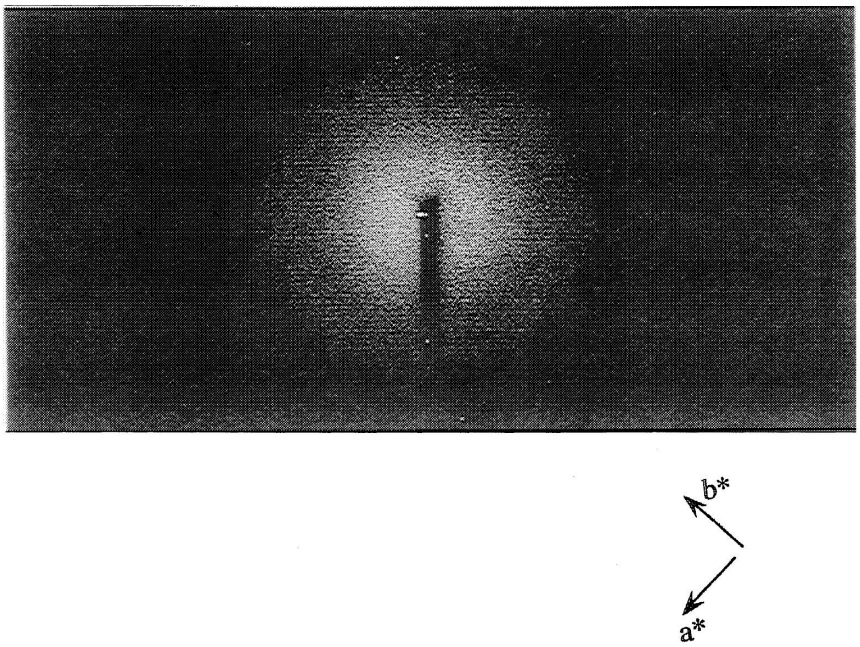

Fig. 3. Synchrotron X-ray Polaroid spots of a micro-single crystal (a few micron) in Phase II powder show a^*b^* plane of the reciprocal lattice.

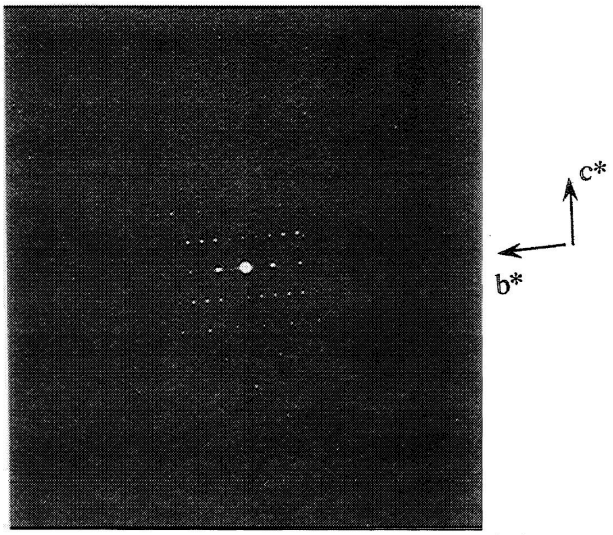

Fig. 4. Electron diffraction photography of b^*c^* plane (Phase II) by TEM (Hitachi H-9000NA), which shows extinction rule of twofold screw axis ($0k0$ $k = 2n+1$).

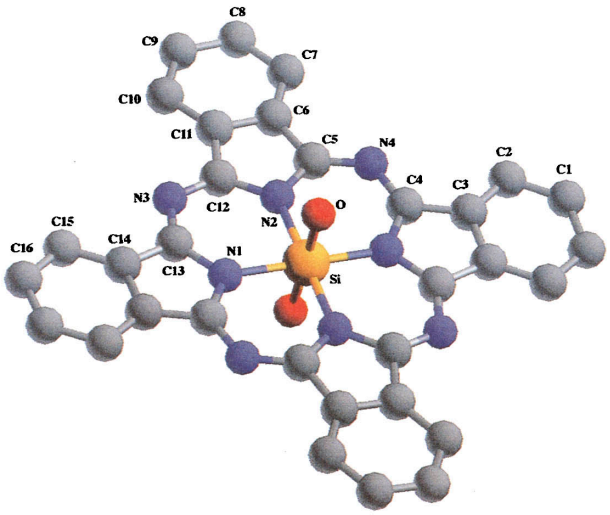

Fig. 5. Molecular structural model determined from the partial coodinates published in Ref. 9. Hydrogen atoms are omitted and the atomic numbering is labeled.

Results and Discussion

Table 4 shows that $Si(OH)_2Pc$, which differs in crystal form (Phase I & Phase II) has very different electric properties. Although Phase II is excellent regarding charge potential, dark decay, sensitivity, and residual potential, Phase I is almost inferior in charge acceptance and cannot actually be used.

Both Phase I and Phase II are dark blue powder. Phase I is more stable than Phase II in solid state because Phase II transforms to Phase I upon strongly grinding for about ten minutes in an agate mortar. The result is shown in Fig. 7. The measured values of the crystal density (Phase I: 1.57

Table 1. Crystal Data and the Final R values

	Phase I	Phase II
Formula	$C_{32}H_{18}N_8O_2Si$	
M.W.	575	
a/Å	12.992(1)	12.7494(5)
b/Å	7.2830(8)	14.5778(6)
c/Å	6.861(1)	6.7727(3)
α/°	104.413(7)	90.0
β/°	101.757(8)	94.353(2)
γ/°	96.973(6)	90.0
Space group	$P\bar{1}$	$P2_1/n$
R_p	0.108	0.093
R_{wp}	0.140	0.126
R_e	0.044	0.037

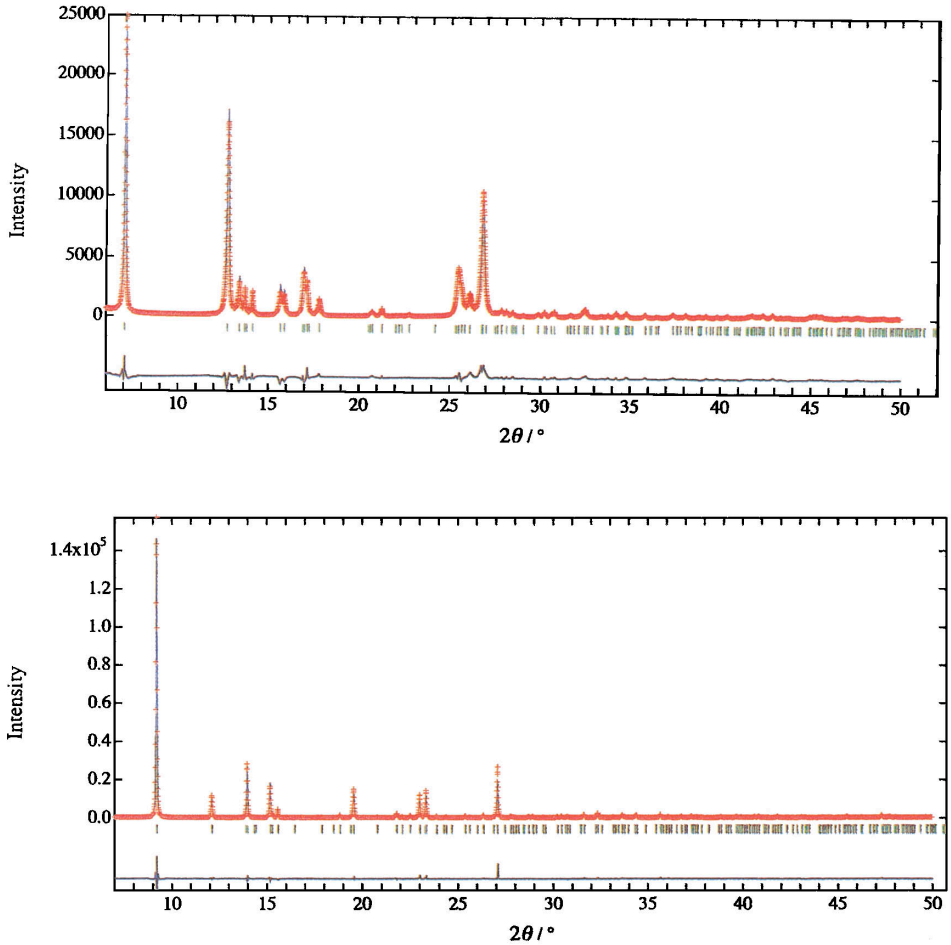

Fig. 6. The results of final Rietveld refinements for Phase I and Phase II with program RIETAN (red: experimental, blue: calculation), with peak markers (green) and difference plot (blue) at the bottom.

Table 2. Atomic Coodinates and Isotropic Temperature Factors (not refined) in Phase I and Phase II

	Phase I				Phase II			
Atom	x	y	z	B/Å^2	x	y	z	B/Å^2
Si	0.0000	0.0000	0.0000	3.0	0.0000	0.0000	0.0000	3.0
O	−0.0270(2)	−0.2096(3)	0.0573(5)	5.0	−0.0795(5)	0.0758(3)	−0.134(1)	5.0
N1	−0.0930(1)	0.1131(5)	0.1594(3)	5.0	−0.1161(6)	−0.0276(5)	0.155(1)	5.0
N2	0.1168(1)	0.0876(5)	0.2434(3)	5.0	−0.0416(5)	−0.0987(4)	−0.179(1)	5.0
N3	0.0310(2)	0.257(1)	0.4956(7)	5.0	−0.1954(8)	−0.1567(7)	−0.029(1)	5.0
N4	0.2586(2)	−0.0391(7)	0.1066(4)	5.0	0.0825(7)	−0.0813(7)	−0.431(1)	5.0
C1	0.3558(4)	−0.341(2)	−0.4539(9)	5.0	0.374(1)	0.059(1)	−0.602(2)	5.0
C2	0.3450(5)	−0.243(2)	−0.2589(7)	5.0	0.2832(9)	0.0076(8)	−0.575(2)	5.0
C3	0.2423(2)	−0.210(1)	−0.2530(5)	5.0	0.2304(9)	0.0244(7)	−0.407(2)	5.0
C4	0.1994(2)	−0.1134(9)	−0.0850(3)	5.0	0.1372(7)	−0.0166(7)	−0.332(2)	5.0
C5	0.2189(2)	0.0508(6)	0.2573(3)	5.0	0.0051(6)	−0.1236(5)	−0.346(1)	5.0
C6	0.2834(4)	0.132(2)	0.4692(6)	5.0	−0.0531(8)	−0.1979(7)	−0.447(2)	5.0
C7	0.3905(5)	0.134(2)	0.5591(9)	5.0	−0.0337(8)	−0.2471(8)	−0.616(2)	5.0
C8	0.4247(5)	0.224(2)	0.7681(7)	5.0	−0.1048(9)	−0.3172(9)	−0.669(1)	5.0
C9	0.3591(5)	0.313(1)	0.8857(6)	5.0	−0.1859(8)	−0.3411(8)	−0.551(2)	5.0
C10	0.2537(4)	0.312(1)	0.7953(5)	5.0	−0.2031(9)	−0.2933(8)	−0.378(2)	5.0
C11	0.2167(3)	0.219(2)	0.5825(4)	5.0	−0.1309(8)	−0.2233(8)	−0.324(1)	5.0
C12	0.1135(2)	0.1916(8)	0.4386(3)	5.0	−0.1283(7)	−0.1553(6)	−0.167(1)	5.0
C13	−0.0651(2)	0.2171(9)	0.3649(5)	5.0	−0.1926(7)	−0.0946(6)	0.113(1)	5.0
C14	−0.1576(3)	0.276(1)	0.4301(6)	5.0	−0.268(1)	−0.093(1)	0.259(2)	5.0
C15	−0.1698(4)	0.3808(1)	0.6202(9)	5.0	−0.357(1)	−0.1457(9)	0.284(2)	5.0
C16	−0.2705(5)	0.409(3)	0.6309(9)	5.0	−0.413(1)	−0.1245(9)	0.448(2)	5.0

Table 3. A Selection of Intermolecular Distances and Angles for Phase I and Phase II; The Atoms of Original Molecule (Left) of Those of the Neighboring Molecule (Right) (Symmetry operations are shown)

Phase I			
	O···N3^{i}	3.18(1) Å	
	C5···C15^{i}	3.47(1) Å	(i) : $-x, -y, -z+1.0$
	C1···C7^{ii}	3.40(3) Å	(ii) : $x, y, z-1.0$
	C2···C7^{ii}	3.32(2) Å	(iii) : $-x, -y+1.0, z+1.0$
	C2···C8^{ii}	3.38(2) Å	(iv) : $x, y-1.0, z-1.0$
	C4···C10^{ii}	3.43(1) Å	
	N3···C15^{iii}	3.37(2) Å	
	N3···C14^{iii}	3.46(1) Å	
	C11···C16^{iii}	3.45(2) Å	
	C12···C15^{iii}	3.25(1) Å	
	C2···C10^{iv}	3.45(2) Å	
	Si–O···N3^{i}	126.0(2)°	
Phase II			
	O···N4^{v}	2.94(1) Å	
	N4···N4^{v}	3.25(3) Å	(v) : $-x, -y, -z-1.0$
	N4···C4^{v}	3.43(2) Å	(vi) : $x, y, z-1.0$
	C2···C12^{v}	3.33(2) Å	(vii) : $x+0.5, y+0.5, z+0.5$
	C4···C5^{v}	3.41(2) Å	
	C7···C13^{vi}	3.45(2) Å	
	C4···C9^{vii}	3.52(2) Å	
	C6···C15^{vii}	3.65(2) Å	
	Si–O···N4^{v}	120.7(3)°	

g cm^{-3}, Phase II: 1.52 g cm^{-3}) support that Phase I is more stable than Phase II. This transition is observed only under mechanochemical process but not in solvents or by heat.

Both of the polymorphous crystals (Fig. 8) have intermolecular hydrogen bonds chains consisting of O–H···N (O···N3 3.18(1) Å for Phase I and O···N4 2.94(1) Å for Phase II). Because in both phases one molecule has two hydrogen bonds using two OH groups and N atoms of the phthalocyanine planes, there is strong intermolecular interaction between the stacks of the phthalocyanine planes. The double hydrogen bonds are along the *c* axis and the molecular interaction continues infinitely along this direction. The hydrogen bond modes of Phase I and Phase II are the same, but the bond distances and angles are slightly different. Table 3 gives the intermolecular distances and angles for Phase I and Phase II. There is π-π stacking interaction between the phthalocyanine planes along the *c* axis in both Phases. The distances between the phthalocyanine planes are 3.3(1) Å for Phase I and 3.2(1) Å for Phase II. The molecules form columns strongly comprising double hydrogen bonds and the π-π stacking interaction. Despite belonging to different crystal systems, there is a clear relation between Phase I and Phase II. The distances of the *c* axes of the two polymorphs are very similar (Phase I: 6.861(1) Å Phase II: 6.7727(3) Å) and there are double hydrogen bonds along the *c* axis in both crystals. The angles of Si–O···N are 126.0(2)° for Phase I and 120.7(3)° for Phase II, and show approximately the same stacking of the phthalocyanine planes. This is best depicted in Fig. 9.

In Phase I the molecular stacking columns are parallel. There is also π–π stacking of the phthalocyanine planes along the *b* axis (Table 3). The distance between the planes is 3.2(1) Å. Along the *a* axis the molecules in Phase I are isolated. It is clear that in Phase I there are double hydrogen bonds and π–π interactions along the *c* axis and another π–π interaction between the phthalocyanine planes in the next translated columns along the *b* axis. However, Phase I has no characteristic interaction along the *a* axis. In Phase II the molecular columns form a herringbone structure with each other led by a two-fold screw axis. The shortest distance between the neighboring columns of the phthalocyanines in the herringbone is about 3.5 Å (Table 3), which suggests that there are some attractive T-interactions between π-electrons and the hydrogen atoms of the phthalocyanine planes (Fig. 10). Thus intermolecular interactions consisting of the hydrogen bonds, π–π stacking interactions and the T-interactions extend in all directions in the crystal. This structure of Phase II is remarkable and could be related to the photochemical sensitivity. The crystal packing is different from those of other phthalocyanines that are hitherto known.[16—20] Furthermore, in Phase I the molecular columns are isolated along the *a* axis, and the feature is particularly different from Phase II.

We compared the crystal structures of the dihydroxysilicon phthalocyanine with those of titanylphthalocyanine (TiOPc). The structures of the two polymorphs (Phase A and Phase B) of TiOPc were determined by the single crystal X-ray method.[16] TiOPc has not symmetry in the molecule because the number of the axial ligands of Ti atom is one, and Ti atom is not located on the center of the phthalocyanine plane. In Phase A, which has some photochemical sensitivity, the neighboring molecules which are related by *c*-glide mirror plane form π–π electron interactions (the distance between the planes is about 3 Å) along the *c* axis. All of the molecules are arranged parallel to *ab* plane and the crystal packing is like a brick. Thus, the intermolecular interactions, which are π–π stacking interactions of the phthalocyanine planes, extend in three dimensions in the crystal. Phase B, which has a slight sensitivity, forms molecular columns with π–π stack-

Table 4. The Results of the Initial Electric Properties for Phase I and Phase II

	Charge potential	Dark decay	Sensitivity	Residual potential
	−V	−V	μJ cm^{-2}	−V
Phase I	150	—	—	—
Phase II	841	26	0.31	13

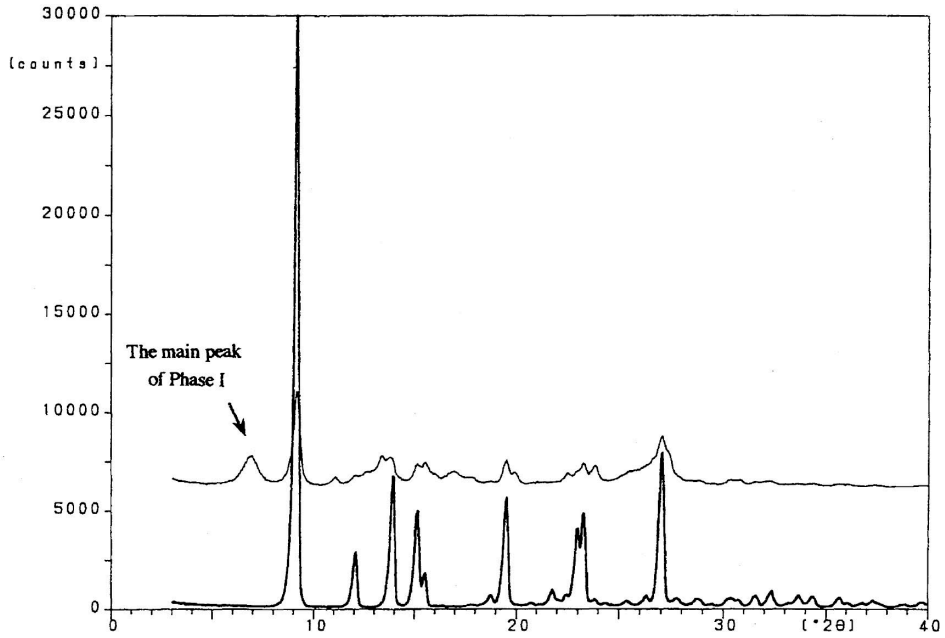

Fig. 7. XRPD data for initial (lower) and after grinding strongly by hand for about ten minuets (upper) in Phase II. The main peak of Phase I appeared by the mechanochemical process. The data were measured using Philips PW1880 diffractometer (Cu $K\alpha$, 40 kV, 30 mA).

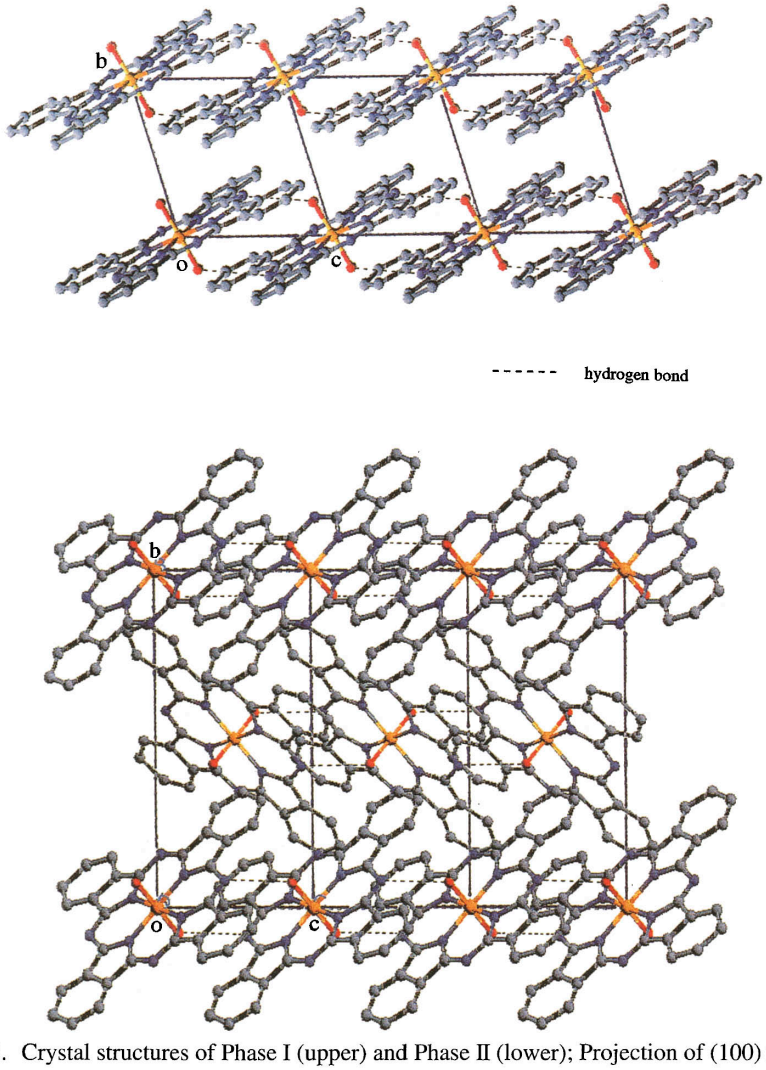

Fig. 8. Crystal structures of Phase I (upper) and Phase II (lower); Projection of (100) face.

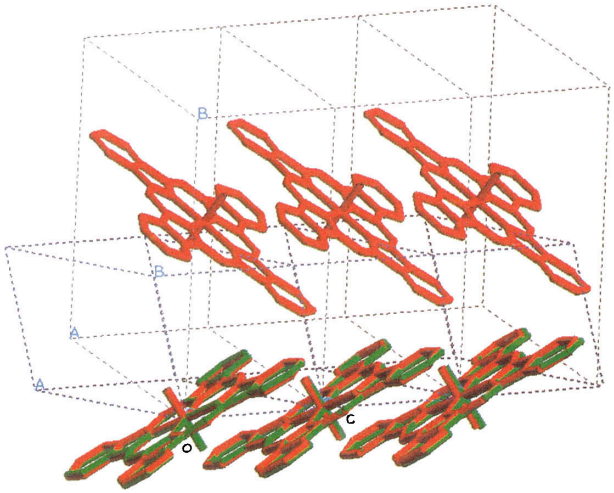

Fig. 9. Crystal structures of Phase I and Phase II that superimposed stacking of the phthalocyanine planes along *c* axis (green: Phase I, red: Phase II).

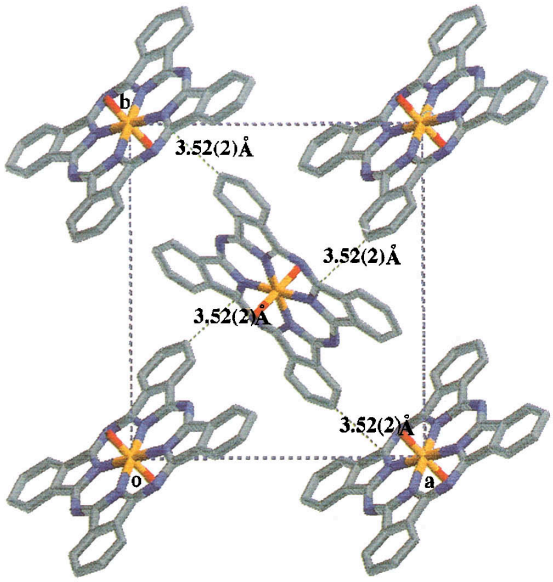

Fig. 10. Crystal structures of Phase II (Projection of (001) face) shows T-interaction.

ing interactions (the distance between the planes is about 3 Å) along the *a* axis. The interactions between the neighboring columns exist, but along the *b* axis very weekly. The strength and extension of the various intermolecular interactions would be closely related to the photosensitivity. We believed that it is important for the system of a charge generation material with proper photochemical activity that in the crystal structure electron flow should not be broken and how easily the electrons flow in all directions in the crystal.

We believe that the kinds of intermolecular interactions such as, hydrogen bonds, π–π electron interaction, and attraction between π-electrons and hydrogen atoms are useful for sensitivity as electrophotographic photoreceptors. It has been shown that when these interactions extend in all directions in the crystal photochemical activity appears. However, it is not clear which one is the most suitable interaction for photochemical sensitivity and the possibility that another suitable interaction exists. To solve these problems, more quantitative analysis of electronic behavior and more crystal structure analyses are necessary.

We thank Prof. Hideo Toraya, Nagoya Institute of Technology for the synchrotron radiation measurement at KEK, Prof. Yuji Ohashi, Tokyo Institute of Technology, for valuable discussions and Dr. Takayuki Shoda for friendly cooperation in molecular mechanics calculation.

References

1 K. Watanabe, A. Kinoshita, N. Hirose, and A. Itami, *Tech. Rep.*, **3**, 108 (1990). [in Japanese]
2 K. -Y. Low, *Chem. Rev.*, **93**, 449 (1993).
3 J. B. Davison and K. J. Wynne, *Macromolecules*, **11**, 186 (1978).
4 K. Oka, O. Okada, and K. Nukada, *Jpn. J. Appl. Phys.*, **31**, 2181 (1992).
5 E. Ciliberto, K. A. Doris, W. J. Pietro, G. M. Reisner, D. E. Ellis, I. Fragala, F. H. Herbstein, M. A. Ratner, and T. J. Marks, *J. Am. Chem. Soc.*, **106**, 7748 (1984).
6 J. W. Visser, *J. Appl. Crystallogr.*, **2**, 89 (1969).
7 A. Boultif and D. Louer, *J. Appl. Crystallogr.*, **24**, 987 (1991).
8 P. -E. Werner, L. Eriksson, and M. Westdahl, *J. Appl. Crystallogr.*, **18**, 367 (1985).
9 J. R. Mooney, C. K. Choy, K. Knox, and M. E. Kenney, *J. Am. Chem. Soc.*, **97**, 3033 (1975).
10 H. M. Rietveld, *J. Appl. Crystallogr.*, **2**, 65 (1969).
11 D. E. Williams, *Acta Crystallogr., Part A*, **A28**, 629 (1972).
12 D. E. Williams, *Curr. Phys.*, **26**, 3 (1981).
13 F. Izumi, H. Asano, H. Murata, and N. Watanabe, *J. Appl. Crystallogr.*, **20**, 411 (1987).
14 F. Izumi, "The Rietveld Method," ed by R. A. Young, Oxford Univ. Press, Oxford (1993), Chap. 13.
15 C. J. Howard, *J. Appl. Crystallogr.*, **15**, 615 (1982).
16 W. Hiller, J. Straehle, W. Kobel, and M. Hanaele, *Z. Kristallogr.*, **159**, 173 (1982).
17 H. Kuppers, W. Kalz, and H. Homborg, *Acta Crystallogr., Part C*, **C41**, 1420 (1985).
18 K. Ejsmont and R. Kbiak, *Acta Crystallogr., Part C*, **C53**, 1051 (1997).
19 T. Inabe and Y. Maruyama, *Bull. Chem. Soc. Jpn.*, **63**, 2273 (1990).
20 B. Boujemaa, M. Ley, and D. Benlian, *Acta Crystallogr., Part C*, **C46**, 379 (1990).